Proceedings of the Estonian Academy of Sciences,
2008, **57**, 3, 179–203
doi: 10.3176/proc.2008.3.07
Available online at www.eap.ee/proceedings

PHYSICS

Long-distance liquid transport in plants

Natalya N. Kizilova

Kharkov National University, Svobody sq. 4, 61077 Kharkov, Ukraine; nnk_@bk.ru

Received 5 May 2008

Abstract. A brief review of the thermodynamic and fluid dynamic problems related to long-distance liquid flow and signalling in plants is presented. Geometrical parameters of the plant leaf venation are measured and the general relationships between the diameters and lengths of the veins, branching angles at the vein bifurcations, and the corresponding drainage areas are obtained. The same relationships had been obtained before for the bifurcations of the pathways in the arterial and bronchial systems of mammals and humans; tree trunks, branches and roots; and river basins. The identity of the principle of design of the transportation systems in the nature can be understood on the concept of optimal networks that provide liquid delivery at total minimal energy costs. The corresponding models of the optimal vessels and branching systems of vessels with impermeable and permeable walls are presented and discussed.

Key words: plant biomechanics, fluid transport, conducting system, optimal pipeline, Murray's law.

1. INTRODUCTION

Living plants receive matter and energy from assimilates (sugars) produced by photosynthetic cells in the leaves. The assimilates are delivered to different parts and organs of a plant as water solutions pumped through special conducting elements (long-distance transport) and by diffusion at the cellular distances (short-distance transport). Though the driving forces and physical mechanisms of the liquid transport and the corresponding thermodynamic models have been discussed in the literature for a long time, many important problems are unexplored and different transport phenomena are not understood yet [32,36]. Plant biomechanics has remained less clear than biomechanics of animals. Because numerous similarities in the geometry, physical mechanisms, principles of construction, and general relationships between the measured physiological and geometrical parameters in high plants and animals are observed, comparative study and analysis of the mechanisms and the corresponding mathematical models are of great interest and importance.

The present review is aimed at deeper consideration of the concepts of an optimal transportation network and a microcirculatory cell in the application to plant biophysics and physiology. Though the construction cost of a plant tissue is sometimes considered as the amount of photoassimilates used for the synthesis of a unit weight of the plant [12], in this paper a general approach based on the energy costs is accepted. It enables comparison of the costs and effectiveness of the construction of similar organs and systems in animals and plants that differ essentially.

2. WATER TRANSPORT RELATIONSHIPS BETWEEN THE SOIL, PLANT, AND ATMOSPHERE

The long-distance transport of liquids in high plants includes the ground water suction by roots; upward transport of the solution (xylem sap) along the xylem pathways from the roots to leaves; water evaporation by the leaves; downward transport of the assimilates produced by photosynthetic cells (phloem sap) along the phloem pathways from the leaves to the growing organs, flowers, fruit, and roots (Fig. 1). The driving forces of the liquid transport are hydrostatic and osmotic pressure drops. The ground water and dissolved mineral substances are transported through the large total surface of the root hairs due to high osmotic pressure maintained by the cells.

Water suction produces a high hydrostatic pressure in the root xylem vessels, which drives the xylem sap against gravity to a certain height, in some instances to the very top of the plant. The hydrostatic pressure decreases with the height of the water columns in the xylem vessels. When the pressure becomes negative, the water column is under tension. The most likely range of negative pressures in xylem is estimated as $P_x = -(0.1–0.6)$ MPa [83].

Two different ways of the small-distance motion of the fluids are present in plants, namely direct intracellular transport through the plasmodesmata (thin channels between the cytoplasmic volumes of the adjacent cells with diameters $d_{pd} = 0.04–0.06$ μm and lengths $L_{pd} = 0.5–1$ μm [1]), which is called symplast transport, and the mass transfer through the cell membranes into the extracellular space and then through the pores of the cell walls (apoplast transport). The total volume of apoplast reaches 10–25% of the leaf volume, forming a significant transportation networks for the water motion into the cells [10]. Conductivity of the apoplast is higher than of the symplast. According to the measurements of the fluid flux J through the apoplast and symplast the relationship between them is $J_a/J_s = 50$.

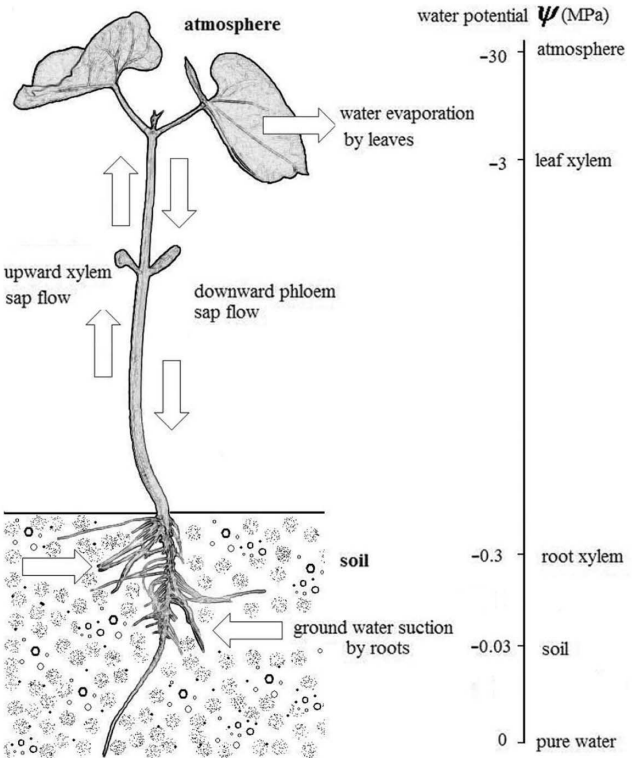

Fig. 1. Water transport relationships between the soil, plant, and atmosphere and the corresponding water potentials.

Radial transport of water in the roots occurs against the friction, which is a dissipative force, so thermodynamic aspects of the water transport from the hair across the root in the xylem vessels are of great interest for both biologists and physicists [24]. The average osmotic pressure in the root cells is $\pi = 0.5$–1.5 MPa, while in the soil it varies from $\pi = 0.3$–0.5 MPa (easily accessible soil moisture) to $\pi = 2.5$–3 MPa (hard-to-reach soil moisture) [64], so the plant adaptation to the local environmental conditions is of great importance for survival and any possible way for optimization of water supply is a key factor for plants.

The root pressure p_r can be measured in the pressure chambers (Fig. 2) by estimation of the outer pressure that is needed to stop the sap outflow from the fresh-cut stalk or stub (Fig. 2, right plant). According to different experiments $p_r = 1$–5 MPa and sometimes it exceeds 5 MPa [64]. The sap moves through the xylem vessels at the rates $V_x = 0.05$–2 m/h in ferns and conifers, 1–6 m/h in foliaceous plants, and 10–60 m/h in grasses, reaching the relatively high velocities $V_x = 20$–60 m/h in some trees and $V_x = 100$–150 m/h in lianas [1].

The conducting pathways form complex branching systems with different geometry and hydraulic properties in stems and leaves (Fig. 3). Xylem conducting elements include tracheids and vessels. Tracheids are elongated, spindle-shaped elements with diameters $d_{tr} = 10$–100 μm and lengths $L_{tr} = 1$–5 mm, which pass water through circular pits in their lateral walls. In comparison with tracheids the vessel elements are wider ($d_{vs} = 20$–800 μm) and have perforated end plates (Fig. 4). They are aligned end to end forming long whole tubes whose length can be comparable to the height of the plant. The butt ends of the vessels are open while tracheids have perforations ($d = 0.1$–1 μm) covered with permeable membranes so that liquid can penetrate through the pores in the membranes. Both tracheids and vessels are formed by cell walls without any live cellular contents, which had been lost at the last stage of development of the conducting elements.

The xylem pathways exhibit some different branching patterns in the roots, stems, and shoots, tree trunks and branches, leaf petioles and blades (Fig. 5). In the leaf blades the conducting vessels produce different complex tree-like branching patterns and networks with numerous loops (leaf venation) and the leaves of different evolutionary age possess different venation types [10]. The total volume of the leaf venation is approximately 10–25% of the leaf volume and the total length of the small veins in a unit leaf area is 20–100 cm/cm^2. The problem and the mechanisms of evolutionary development of the conducting

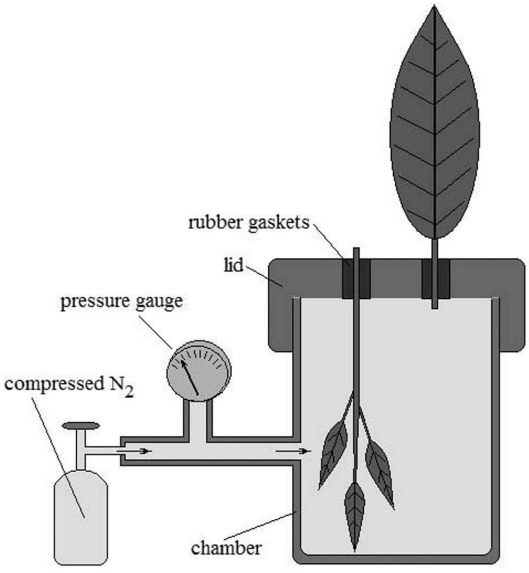

Fig. 2. Measurement of the water potential of plants in the pressure chamber.

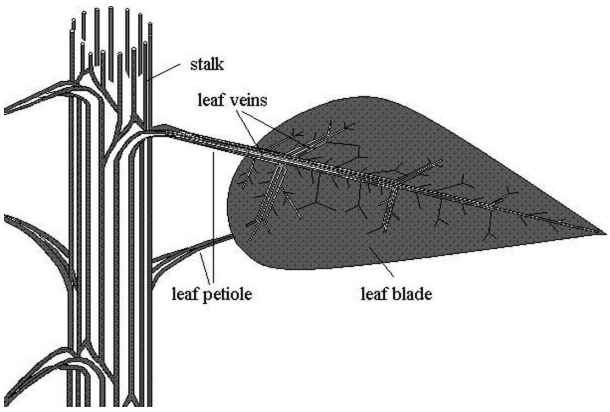

Fig. 3. Water conducting system of a plant.

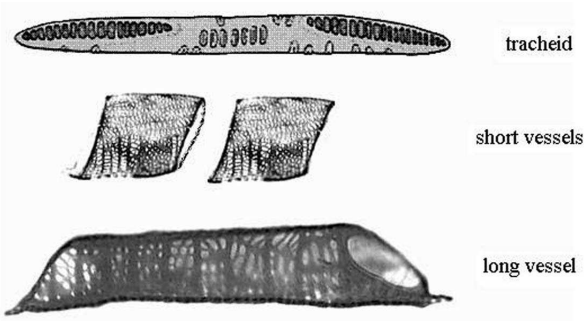

Fig. 4. Conducting elements of plants.

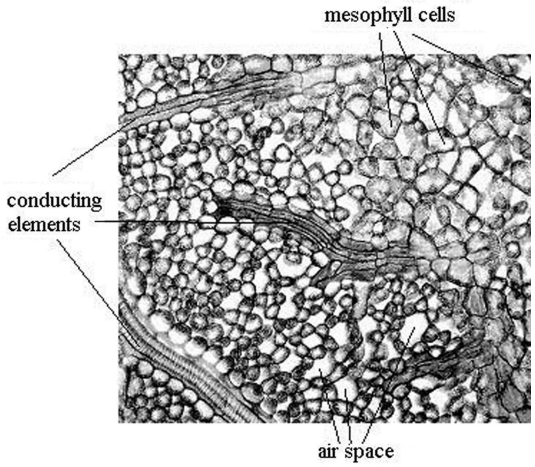

Fig. 5. Xylem pathways and mesophyll structure.

systems in plant stems, roots, and leaves are widely discussed in the literature [10,42,64]. For instance, significant evolutionary correlations between the leaf-specific xylem hydraulic conductivity, leaf venation density, leaf size, and some other indices as well as between the stem and leaf conducting systems have been found [8,54].

Only a small amount of water (approximately 1–2% [42,64]) received by leaves is used for the photosynthesis and production of sugars. The rest of the water is evaporated in the atmosphere and therefore is used for driving the upstream flow, which is the unavoidable cost for the long-distance transportation. The energy for the evaporation process comes from the sun that provides the energy to overcome the latent heat of evaporation of the water molecules. Water evaporation in the leaves results in negative pressures $P_{\mathrm{l}} = -2$–1 MPa, which are produced by the surface tension at the total surface of the water meniscus at the terminuses of numerous xylem elements with diameters $d_{\mathrm{m}} = 10$–50 μm, which are open inside the leaves (Fig. 5). The pressure drop $\delta P = P_{\mathrm{r}} - P_{\mathrm{l}}$ is sufficient for lifting the water up to the top of the high trees (100 m and even higher).

The negative pressure at the upper end of the xylem causes high tension of the liquid contents of the xylem pathways (water threads), so the problems of gas bubble formation and cavitation arise and are not solved yet, because the pathway can be occluded by the bubble and in that way damaged as a sap conductor [18]. Cavitation is regarded as a factor that limits plant growth and productivity and, hence, competitiveness for light and nutrients [90]. The most fundamental effects of embolism on the sap flow are decrease in permeability [48] and release of water from embolized conduits to the transpiration stream that can be indirectly detected by observing variations in the diameter of the stalk [19].

A suggestion that the occluded xylem vessel is damaged forever and other pathways will be formed during the future plant growth and morphogenesis is discussed in the literature [42,64]. However, the bubbles can be removed from the pathways, which can be refilled as it was shown by acoustic detection [89] of the bubble cavitation and noise generation in the tree trunks and branches, especially in springtime after the sap flow has decreased or completely stopped for the wintertime [3,95]. Some biophysical and thermodynamic mechanisms of bubble formation and removal are presented in the literature, but the question still remains open [45,95].

The photosynthetic cells in leaves and shoots contain a sugar-rich solution with a high osmotic pressure. The cells can contact with xylem vessels through a semipermeable membrane that allows water transfer but does not transmit assimilates. Then the phloem sap (a sugar-rich solution) moves through the phloem vasculature, which is composed of sieve elements and companion cells. In contrast to the xylem conducting elements, the sieve elements are living cells of 20–30 μm in diameter and 100–150 μm in length separated

by the sieve plates and aligned side by side in parallel with xylem vessels. Because the membranes of the adjacent cells are joined together through small perforations in the sieve plates, the cells can communicate directly via mass transfer between the intracellular spaces.

While the phloem sap moves along the phloem pathways, the sugars are absorbed by living cells (active mass transfer through the cell membranes) and concentration of assimilates becomes lower than generates a concentration gradient along the phloem pathways. The representative value of the phloem flow rate is $V_{\text{ph}} = 0.05$–1 m/h [64].

3. BIOPHYSICAL THEORIES OF WATER MOTION AND EXCHANGE IN PLANTS

The simplest lumped-parameter models describing the pressures in different compartments (soil, root, xylem, phloem, leaf, and atmosphere) and the fluxes of water and substances between them are useful for rough estimations and are based on the dependences between the fluxes and pressures in the compartments [27].

The most accepted theory of water motion in the xylem pathways is the cohesion–tension theory proposed by Dixon and Joly in 1895 [7]. It is based on the idea of cohesion forces between the water molecules; the forces are supposed to be strong enough to provide continuity of the water threads even at high tension. A quantitative basis was developed by van den Honert in 1948, who proposed an Ohm's law analogue as a relationship between the flow and the pressure gradient [94]. According to the cohesion–tension theory, water ascends plants in a metastable state under tension when the xylem pressure is more negative than that of the vapour pressure of water.

The negative pressure is generated by surface tension at the evaporating surfaces of the leaf and then is transmitted through a continuous water threads from the leaves to the roots and throughout the apoplast in every organ of the plant. Evaporation creates a curvature in the water menisci within the cellulosic microfibril pores of cell walls and at the outlets of the xylem terminuses. As a result the xylem pressure becomes lower directly behind the menisci (at the air–water interfaces) due to surface tension [91].

Mathematical modelling of xylem flow is usually based on the 1D momentum equation for an incompressible viscous fluid in the long cylindrical tube of radius R and length L [67]:

$$\frac{\mu}{r}\left(\frac{1}{r}\frac{\mathrm{d}v(r)}{\mathrm{d}r}\right) = \frac{\mathrm{d}p(x)}{\mathrm{d}x} + \rho g, \quad v|_{r=R} = 0,\ p|_{x=0} = P_{\text{r}},\ p|_{x=L} = P_{\text{l}},$$

where $P_{\text{r,l}}$ are pressures in the root and leaves.

Another approach in modelling the xylem transport in plant tissues is based on the fluid percolation in a non-uniform anisotropic porous medium, which is propelled by the gradient of water potential. The governing equation is [2]:

$$C_V \frac{\partial \Psi}{\partial t} = \operatorname{div}(k\nabla\Psi) - \alpha(\Psi - \Psi_v) - \varepsilon(t)S(x),$$

where $C_V = \frac{1}{V}\frac{\partial V}{\partial \Psi}$ is the normalized capacity, Ψ and Ψ_v are water potentials in the tissue and in the xylem vessels, $\varepsilon(t)$ is transpiration rate, $S(x)$ is the total leaf surface, α is the resistivity of the vessel to medium water pathways, and $k = k(x,\Psi)$ is permeability.

In 1930 Münch proposed his famous hypothesis on the sap flow in the phloem [58]. He suggested that the xylem and phloem conduits are couples like two osmometers submerged into the tanks with the solution of concentration C_0, which is a model of plant apoplast (Fig. 6). The left osmometer represents the photosynthetic leaf, which is filled with a concentrated sugar solution (concentration C_1). The right osmometer represents any organ working as a sink for the assimilates and the sugar concentration in it is $C_2 << C_1$. The two osmometers are connected by a long tube modelling the phloem pathway. The semipermeable membranes of the two osmometers are supposed to be of the same permeability, so the water will be osmotically driven inside the right osmometer, which will increase the hydrostatic pressure P_{l}

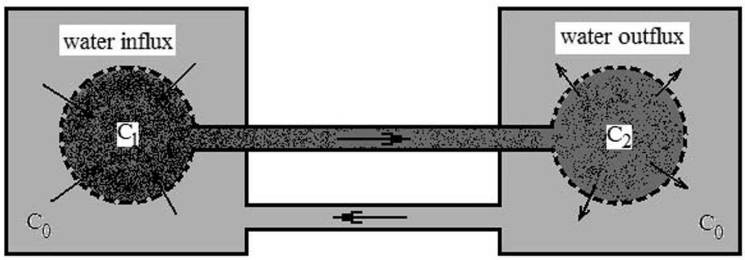

Fig. 6. Münch's model of the phloem transport.

in it and will cause the flux of the solute through the tube. The interconnection of the osmotic and hydrostatic pressures in the liquid pumping in plants is similar to the interconnection of the hydrodynamic pressures in the heart atriums and ventricles, so Münch's hypothesis describes the pumping 'heart of the plant' [25].

The unified approach to the mathematical description of water motion in plants is based on the water potential Ψ, which is the potential of the solution relative to pure water $\Psi = (\mu - \mu_0)/V_0$, where μ and μ_0 are chemical potentials of the solution and water, respectively, and V_0 is the partial molar volume of water. The water potential can be considered as a sum of the components $\Psi = \Psi_\pi + \Psi_p + \Psi_m + \Psi_\chi + \Psi_g$, where π, p, m, χ, g correspond to osmotic, hydrostatic (due to the intracellular turgor pressure), matrix (interaction with molecular structures and surfaces), humidity, and gravitation potentials. The matrix potential is of great importance in soils, cell walls, and water–air interfaces where the surface forces and related surface phenomena are essential, while the gravitation potential is important for the high plants. The chemical potential of the sap is a function of the temperature, hydrostatic pressure, and molar concentrations of water N_w and the dissolved components N_j, $j = 1...n$: $\mu = \mu(T, p, N_\mathrm{w}, N_j)$. In that way

$$\mathrm{d}\mu = \frac{\partial \mu}{\partial T}\mathrm{d}T + \frac{\partial \mu}{\partial p}\mathrm{d}p + \frac{\partial \mu}{\partial N_\mathrm{w}}\mathrm{d}N_\mathrm{w} + \sum_{j=1}^{n}\frac{\partial \mu}{\partial N_j}\mathrm{d}N_j, \tag{1}$$

where all the derivatives are taken keeping the other independent variables as constants.

Since $\frac{\partial \mu}{\partial p} = V$, $\frac{\partial \mu}{\partial N_j} = -V_0 \mathrm{d}\pi_j$, where V is the partial molar volume of the dissolved components, π_j is the partial osmotic pressure, and $\mu_j = \mu_j^0 + RT\ln\left(p_j/p_j^0\right)$, where p_j is the partial pressure of the j-th component over the solution at given p and T and p_j^0 is the pure pressure of the j-th component. Raul's law for an ideal solution stands $p_j = N_j p_j^0$, so $\mu_j = \mu_j^0 + RT\ln\left(p_j/p_j^0\right) = \mu_j^0 + RT\ln N_j$ and the following relationship can be obtained from (1) at $T = \mathrm{const}$ [82]:

$$\mathrm{d}\mu = V_0\mathrm{d}p - V_0\mathrm{d}\tau - \sum_{j=1}^{n} V_0\mathrm{d}\pi_j, \tag{2}$$

where $\pi_j = -\frac{\mu(N_j)-\mu_j^0}{V_0}$ is the partial osmotic pressure produced by the j-th dissolved component and $\tau = -\frac{\mu(N_\mathrm{w})-\mu^0}{V_0}$ is the matrix pressure.

Upon integrating (2) at $V_0 = \mathrm{const}$ (for the dilute solutions $V_0 \approx 18$ cm^3/mol [107]) one can obtain $\Psi = p - \pi - \tau \equiv -S$, where $S > 0$ is the sucking force and p is the hydrostatic pressure relative to the atmospheric pressure.

Water potentials of the leaves, small shoots, and seedlings can be measured in the pressure chambers (Fig. 2, left plant). The method was pioneered by Dixon at the beginning of the 20th century [6] and introduced into widespread practice by Scholander and coworkers [76]. In the method, the excised sample is sealed into the chamber leaving the cut-off outside the chamber. After the excision the water column

in the xylem, which had been under tension, is broken and the water is sucked by the surrounding cells due to osmosis. In the course of the measurements one has to pressurize the chamber with compressed gas until the water meniscus is detected at the outlets of the xylem vessels. The pressure needed to lift the water back is called the balance pressure and is regarded as a measure of the water potential in the sample measured in MPa. Some other methods based on the pressure microsensors and osmometers have also been developed. The measurements give different values for the water potentials in the leaves ($\Psi = -1$–1.2 MPa [11], $\Psi = -0.7$–1 MPa [91], $\Psi = -0.58$ MPa [98]) and roots ($\Psi = -0.2$–0.3 MPa [91]) of different plants, and of the soils ($\Psi = -0.03$–0.05 MPa [91]). The water potential undergoes diurnal variations due to different temperatures, sun radiation, and transpiration rates. For instance, the daily variations $\Psi = -1$–2 MPa have been measured in a pine at the same height. At night, when transpiration is minimal, the water potential in mature maize leaf was $\Psi = -0.12$ MPa, which is almost in equilibrium with soil ($\Psi = -0.08$ MPa). In the elongating part of the growing leaf $\Psi = -0.5$–0.55 MPa, which promotes high turgor pressure for subsequent leaf growth [98]. Delivery of water, mineral elements, and assimilates inside the plant is determined by the gradients of water potential between the roots and stem and stem and leaves. In rapidly elongated oat coleoptiles $\delta\Psi = 0.25$ MPa [98]. In some lianas $|\nabla\Psi| = 0.08$ MPa/m along the stem and branches, $|\nabla\Psi| = 0.27$ MPa/m between the stem and leaves, and $|\nabla\Psi| = 0.2$ MPa/m at branch junctions [11].

Basing on the concept of the gradient of water potential as a driving force for the sap flow, the hydraulic resistivity Z of a plant or its any part can be introduced as $Z = \left(\Psi_{\text{soil}} - \Psi_{\text{leaves}}\right)/J_{\text{w}}$, where J_{w} is the total water flux measured in the stalks by flowmeters or by water evaporation rate. The Poiseuille law of the incompressible viscous flow is usually considered and the hydraulic resistance of a single conducting element (both tracheids and vessels) is calculated as $Z_{\text{P}} = 128\,\mu L/\left(\pi d^4\right)$, where L and d are the length and diameter of the conducting element, μ is the fluid viscosity. Resistivity of a bunch of tubes and a bifurcation of conducting elements is calculated then as parallel and series connections of the tubes with known resistivity. Validity of Poiseuille's law for the plants has been thoroughly verified and the hydraulic resistivity of real conducting pathways was found to be bigger than the theoretical values, namely $Z = aZ_{\text{P}}$, where $a = 2.04$ for lianas [11]. The main resistive part of the xylem pathways is presented by perforation plates between the vessels and tracheids. The pressure gradient within the pores of the plate is about 40-fold greater than that for the open part of the pathway [78]. Both experimental measurements and FEM calculations of the resistivity of the series connection of two tubes with a 20-pores perforation plate between them revealed that the plate contributes 21–23% of the total flow resistance depending on the angle between the plate and the axis of the tube [78]. The hydraulic architecture of different plants has been intensively studied in a wide range of experimental and theoretical papers.

The conducting pathways in the leaf constitute a substantial ($\sim$30%) part of the resistance to the water flow through the plant [75], and thus influence photosynthesis and transpiration and correlate with regeneration irradiance in trees [73]. Leaf hydraulic resistivity varies more than 65-fold across species, which reflects differences in the venation architecture. Some leaf traits are independent of hydraulic resistivity, including area, shape, thickness, and density, demonstrating that leaves can be diverse in gross structure without intrinsic trade-offs in hydraulic capacity [74]. Detailed electronic circuit models of the leaf hydraulic architecture as a network of resistors with distinct resistivity for mesophyll cells and veins of different conductivity have been studied [72] to understand leaf hydraulic design. The total conductance of a tree or a shoot is calculated as the result conductance of the root, stem, branches, and leave in a series and parallel connection in accordance with tree geometry [91]. Hydraulic models of trees, roots, and leaves are of great interest for plant physiology and agriculture [51,61,79]. Hydraulic approximation is found to be useful for general description of liquid transfer between different conducting elements and organs.

Within the framework of the cohesion–tension theory the pressure gradient in the plant is estimated from the balance equation [91]:

$$\frac{\mathrm{d}P}{\mathrm{d}x} + \rho g \frac{\mathrm{d}h}{\mathrm{d}x} + \frac{S\varepsilon}{L_h} = 0,$$

where ε is the relative transpiration rate at the terminus of the branch with total leaf surface S and hydraulic conductivity L_{h} at the height h. If the transpiration rate and the pressure difference at the ends of a branch of length L are measured, the expression for the hydraulic conductivity can be obtained in the following form:

$$L_{\mathrm{h}} = \frac{SL\varepsilon}{\Delta P - \rho g \Delta h}.$$

Most thermodynamic considerations of the liquid transport in xylem and phloem are based on the model of the xylem vessel containing pure water or a weak solution of an osmotically active component, living cells, and phloem cells with their sugar-rich contents, where the sugar solution and water are separated by a semipermeable membrane [23–25,45]. The xylem pressure can be controlled by the rates of water transpiration by leaves and suction by roots. Minimizing the Gibbs energy function for the system xylem–semipermeable membrane–phloem the vapour pressure and osmotic pressure equations were derived in the form [45]:

$$v_{\mathrm{w}}(p - p*) + \gamma a + \gamma_c a_c = RT \ln \frac{p_{\mathrm{v}}}{p*}, v_{\mathrm{w}}(p - p_{\mathrm{s}}) + \gamma a + \gamma_c a_c = RT \ln \alpha_{\mathrm{ws}},$$

where p, p_{v}, $p*$, p_{s} are xylem, vapour, saturated valour, and solution pressures, $\gamma(T)$ is the free energy of the water–air interface, $\gamma_c(T)$ is the free energy difference of the wetted and dry water–solid surface, a and a_c are specific interface areas, α_{ws} is the activity of water in the sugar solution. As it was shown by numerical estimations on the obtained formulae, when the gas bubbles appear in the xylem pathways, the air–water interface area and the surface energy become bigger, diminishing the pressure of water. Cavitation of the bubbles produces an additional suction pressure for the xylem water [45].

Münch's model of the phloem sap motion has been revisited basing on the thermodynamic relationships between the forces and fluxes [16,23]. The flux of the plant sap J_x is determined by the hydrostatic, osmotic, and matrix pressure gradients

$$\vec{J_x} = L_{\mathrm{h}}(\nabla p + \sigma \nabla \pi + \nabla \tau), \tag{3}$$

where L_{h} is hydraulic conductivity of the conducting ways, $0 < \sigma < 1$ is the reflection coefficient.

Expression (3) at $\nabla \tau = 0$ was hypothesized by Starling in 1896 in application to the fluid flow out of the blood capillaries and its thermodynamic substantiation was given by Kedem and Katchalsky [28]. For the plant assimilates (sugar solution) $\sigma = 0.7$–0.8 [82]. The water flux in the roots $\vec{J_r} = L_{\mathrm{h}} \sigma \nabla \pi + \vec{\Phi}$, where $\vec{\Phi}$ is the energy-dependent metabolic component of the flux that remains nonzero when $\nabla \pi = 0$ [107].

Mathematical description of Münch's model is based on the Navier–Stokes equations of the low-Reynolds laminar flow in the long tube [67] or the fluid filtration in the porous medium according to the Darcy law:

$$\vec{v} = -\frac{k}{\mu}(\nabla p + \rho \vec{g}), \tag{4}$$

where k is the permeability of the plant tissue. According to the measurements on the pine trees $k = (1{-}4) \cdot 10^{-12} \mathrm{m}^2$ [45].

A hydrodynamic model of the phloem transport as a fluid flow in a long tube is studied in [16,38]. The governing equations are Navier–Stokes equations of the fluid motion due to the osmotic pressure gradient, the van't Hoff equation for a dilute solution, and the diffusion equation for the dissolved osmitically active substance:

$$\rho \frac{\mathrm{d}\vec{v}}{\mathrm{d}t} = -\nabla p + \mu \Delta \vec{v}, \;\; p = p_0 + \pi, \;\; \pi = RTC, \tag{5}$$

$$\frac{\partial C}{\partial t} + \mathrm{div}(\vec{v}C) = 0, \tag{6}$$

where C is concentration, π is osmotic pressure, p and p_0 are hydrostatic pressures in the tube and in the surrounding medium, ρ is density, and $\vec{v}$ is velocity of the phloem sap.

The steady-state solution ($\vec{v} = v_x(r)\vec{e}_x$) has been obtained in analytical form and the time-dependent solution has been computed numerically at the following boundary conditions:

$$C|_{x=0} = C_0, C|_{L=0} = C_L. \tag{7}$$

At dynamic equilibrium the concentration gradient between the inlet and outlet of the tube that is maintained by active synthesis (absorption) of the dissolved component in different vegetative organs of the plant defines the propelling force of the fluid flow. As it was shown by calculations, the radial and longitudinal transport of water and substances in the phloem tube are coupled and complex nonlinear concentration profiles along the tube may appear at different values of the model parameters.

The system soil–plant–atmosphere is interconnected by means of the water threads in the xylem vessels so any disturbance in the atmosphere (CO_2 concentration, temperature, humidity, mixing of the boundary layer by the wind) and in the soil (temperature, salinity) produces a fast reaction of the plant [43,46,107]. Rapid variations of osmotic pressure of the root solution cause quick alterations of the stem diameter produced by changes in the leaf transpiration rate. Diameter alterations have been observed at rather small variations of the concentration ($C \sim 0.01$) and they outrun the bioelectric reaction, which is noticeable at $C \sim 0.3$–0.5 only. The alterations of the stem diameter propagate along the stem in a wave-like way with velocity $v \sim 0.1$–1 m/s, which considerably exceeds the fluid flow along the stem ($v \sim 10^{-4}$ m/s). The explanation of the quick reaction of the plants may be given basing on the model of the pressure wave propagation in plant tissues as saturated porous media [26,27]. Similar slow waves with $v \sim 96$ cm/s have been revealed in experiments [97].

A possible mechanism of the long-distance high-speed signalling in high plants can be connected with concentration waves propagating along the vessels [38]. As the pressure and concentration are related by the van't Hoff equation, one can speak about the pressure–concentration waves. Concentration waves can be produced by variation of the value C_0 in (7). The steady solution of the problem (5)–(7) determines the parabolic velocity profiles and nonlinear concentration distribution for the stationary flow. The wave velocity range $U = 20$–60 m/s, obtained by numerical calculations on (5)–(7), corresponds to the measured time delay. For the length $L_\Sigma = 0.1$–1 m of the plant the time delay between the moment of rapid concentration variation in the soil and the reaction of the distant leaves is $t \sim 1.7$–50 ms, which is comparable to the experimental values [27]. In that way the concentration waves can mediate long-distance high-speed transfer of information between the organs that can not be carried by the convective flow of the sap ($V \sim 10^{-5}$–10^{-4} m/s).

The pressure–concentration waves have also been studied on equations (4) and (6) for the rigid tube [86] and when the tube elasticity is taken into consideration, so the tube lumen area S is allowed to vary according to the pressure difference:

$$\frac{\partial S}{\partial t} + \frac{\partial Sv}{\partial x} = SL_\mathrm{h}(\Psi_0 - p - \pi), \tag{8}$$

where $v = -\frac{k}{\mu}\frac{\partial p}{\partial x}$, x is the axial coordinate. The sieve tube permeability has been calculated as a series connection of the Poiseuille conductivity of the sieve cell with length l and diameter d and the sieve plate composed of parallel connection of N pores with diameters d_p and lengths l_p, so

$$k = \left(\frac{8Nd_\mathrm{p}^4 l}{8Nd_\mathrm{p}^4\left(l - l_\mathrm{p}\right) + \left(8l_\mathrm{p} + 3r_\mathrm{p}\right)d^4}\right)\frac{d^2}{32}$$

and the volumetric elastic modulus of the tube has been introduced as $E = S\,dp/dS$. The equations for pressure and concentration have been obtained from (6) and (8) and studied in [83].

It was shown that the speed of propagation of pressure–concentration waves is not significantly impeded by wall elasticity, but rather by the ratio of sap osmotic pressure to the axial drop in sap hydrostatic pressure.

The results permit future theoretical basis to the 'osmoregulatory flow' hypothesis [85], which argues that efficient molecular control of the phloem is possible by maintaining the sieve sap hydrostatic pressure at a value that is spatially nearly constant, which in turn permits changes in sieve tube state to be rapidly transmitted throughout the sieve tube via pressure–concentration waves [83].

Water evaporation (transpiration) rate is determined by the vapour concentration at the surface–air interface c_w and in the atmosphere c_a and by the total resistivity R_Σ of all the vapour pathways (inside the leaf, through the epidermis, and through the adjacent air layer) as [65,82]:

$$\varepsilon = \frac{c_w - c_a}{R_\Sigma} = \frac{273\rho_w}{P_a T}\frac{p_w - p_a}{R_\Sigma},$$

where ρ_w is the vapour density, P_a and T are atmospheric pressure and temperature, p_w and p_a are pressure of vapour over the transpiration surface and in the atmosphere. According to Raoult's law the vapour pressure of an ideal solution depends on the vapour pressure of each chemical component and the mole fraction of the component present in the solution, so

$$\frac{p_0 - p_w}{p_w} = \frac{\nu_s}{\nu_f},$$

where ν_s and ν_f are mole fractions of the component and the solvent (water), p_0 is vapour pressure over pure water, so that $p_w = p_0\nu$, where $\nu = \nu_f/(\nu_s + \nu_f)$ is a mole fraction of water. This model has been used together with diffusion equations for a dissolved component, and the concentration of the component is determined by the transpiration rate and consumption of the component by cells [40]. In the lumped parameter models some simple approximations of the transpiration rate are introduced, for instance [65]:

$$\varepsilon = \rho_a \vartheta \frac{\beta_w(T) - \beta_0(T)}{R_2 + R_3},$$

where $\beta_w(T)$ is the air humidity in the air space inside the leaf, $\beta_0(T)$ is the air humidity in the atmosphere, T is the temperature, $R_{2,3}$ are hydraulic resistivity of the stomata and the adjacent air layer, ρ_a is the air density, ϑ = const is a geometric coefficient. Some approximations for $\beta_w(T)$ and dependence of R_3 on the wind velocity can be found in the literature [106].

For the 2D problem of water diffusion inside the air space of the leaf and water evaporation at the leaf surface, some empirical approximation has also been used [62]:

$$\varepsilon = \frac{k_1 D}{k_2 D + k_3 + h} + k_4,$$

where $D = D_e/D_i$ is a ratio of the diffusion coefficients of the vapour at the leaf surface and in the air space, k_{1-3} are empirical parameters.

Investigation of the interconnection between the water suction and radial transport in roots, xylem sap flow due to the hydrostatic pressure drop, water evaporation in the leaves, sugar production by the photosynthesizing cells, motion of the phloem sap along the phloem vessels due to the osmotic pressure drop, absorption of the assimilates, which makes a closed circle of the water exchange in the whole plant, is far from completion and understanding and poses a set of challenging problems for modern biophysics, thermodynamics, and mathematics.

Because hydraulic architecture determines the water flux and transport efficiency in plants, optimization of the vascular system towards minimization of its total hydraulic resistivity is an important problem, which was raised in connection with optimal transport properties of the long-distance fluid transportation systems in animals [68].

4. THE CONCEPT OF AN OPTIMAL TUBE AND BIFURCATION OF TUBES

The very first observation of the regularities in the structure of the circulatory system in humans was presented by German physician Wilhelm Roux in his doctoral thesis in 1878. He supposed that the physical forces rather than genetic or regulatory factors influence the form of bifurcations, imposing constraints on their shape and function that are interconnected by general physical laws. Roux formulated his bifurcation rules in the following form:

When the parent vessel with diameter d_0 is divided into two daughter vessels with diameters d_1 and d_2 possessing the branching angles α_1 and α_2 respectively (Fig. 7a), then
(1) $\alpha_1 \approx \alpha_2$ if $d_1 \approx d_2$;
(2) $\alpha_1 > \alpha_2$ if $d_1 < d_2$;
(3) $\alpha_1 \approx 90^\circ$ if $d_1 << d_0$;
(4) $\alpha_2 \approx 0^\circ$ if $d_2 \approx d_0$.

As the regularities had been observed in vast measurements on the arterial vasculatures of mammals and humans, a concept of optimal construction of the blood vessel networks was proposed. The mathematical problem of the optimal branching delivering the blood along the series connection of the tubes AB and BC to the inner organ C (Fig. 7b) was solved by Lighthill, who considered the total hydraulic conductivity Z as a minimizing function [47]. When the blood motion is considered as a steady fully developed flow of a Newtonian liquid, the total hydraulic conductivity can be calculated as

$$Z_{\mathrm{ABC}} = Z_{\mathrm{AB}} + Z_{\mathrm{BC}} = k\left(\frac{h \cdot cth(\theta_0)}{d_0^4} + \frac{h(cth(\theta_0) - cth(\theta))}{d_1^4}\right),$$

where $k = 8\mu/\pi$, μ is fluid viscosity.

The problem $Z_{\mathrm{ABC}}(\theta) \to \min$ has the only solution $\cos(\theta) = d_1^4/d_0^4$, which corresponds to the measurement data obtained on the arterial bifurcations of muscles, brain, heart, lungs, mesentery, kidneys, and other internal organs [22,50,55,66,80,101–104]. The same optimization problem was solved for the optimal bifurcation (Fig. 7a) and the relationships between the optimal branching angles and the diameters were obtained in the form [71]:

$$\cos(\alpha_{1,2}) = \frac{d_0^4 + d_{1,2}^4 - d_{2,1}^4}{2d_0^2 d_{1,2}^2}. \tag{9}$$

Another regularity has been obtained on a huge amount of statistical data measured on the X-ray images and plastic casts of the vasculatures in a general form

$$d_0^\lambda = d_1^\lambda + d_2^\lambda, \tag{10}$$

where λ is close to 3. A theoretical explanation of (10) was proposed by Murray in 1926 [59,60] based on the optimality principle for a single blood vessel, which had been treated as a rigid circular cylinder. The

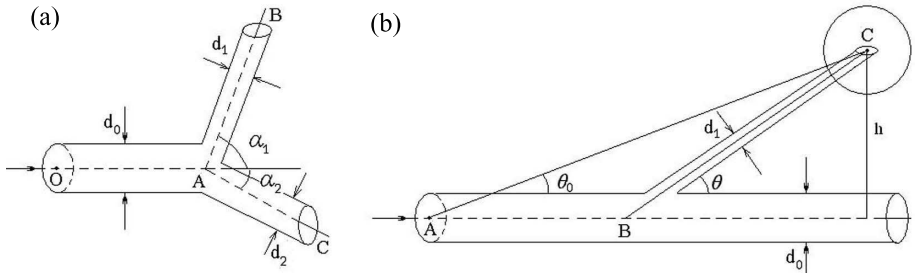

Fig. 7. Arterial bifurcation (a) and branching (b).

total energy W expended on the fluid flow, tube wall construction (construction costs), and nutrition and the energy consumption for the fluid nutrition (blood oxygenation and other metabolic costs) was proposed as an optimization criterion in the form

$$\dot{W} = Q^2 Z + \kappa V \to \min, \tag{11}$$

where $Q^2 Z$ is the viscous dissipation, V is the volume of the tube (including the inner volume and the wall volume), and κ is a metabolic constant.

The solution of problem (11) gives $Q^2 = \beta^2 d^3$, $\beta = \pi/32\sqrt{\kappa/\mu}$ for the optimal tube. From here one can easily obtain Murray's law for the flow through the bifurcation of the optimal tubes when $Q_0 = Q_1 + Q_2$

$$d_0^3 = d_1^3 + d_2^3, \tag{12}$$

which is sometimes called a Pythagorean Theorem in physiology.

Since problem (11) has the same solution as the optimization problems

$$Q^2 Z \to \min \text{ at } V = \text{const and } V \to \min \text{ at } Q^2 Z = \text{const},$$

the optimal pipeline constructed basing on Murray's law possesses minimal hydraulic resistance at a given volume or a minimal volume at given energy expenses, so the existence of the sort of optimal conducting systems is intuitively clear.

If the bifurcation is optimal and the branching angles are described by (9) and Murray's law for the diameters is valid, relationship (9) can be rewritten in a convenient form using the asymmetry coefficient $\xi = \min\{d_1, d_2\}/\max\{d_1, d_2\}$, namely:

$$\cos(\alpha_1 + \alpha_2) = \frac{\left(1+\xi^3\right)^{4/3} - \xi^4 - 1}{2\xi^2}. \tag{13}$$

The mechanism of the formation of the optimal branching pipelines that correspond to Murray's law is obvious, because for the Poiseuille flow the shear rate at the wall is $\tau_w = 32\mu Q/\left(\pi d^3\right)$, so in the optimal tube $\tau_w = \text{const}$. In that way when in a growing body the shear stress at the vessel wall is kept at a prescribed level $\tau_w = \text{const}$, the optimal tube (in the meaning of the optimization criteria (11)) will be developed. The mechanism definitely exists in the blood vessels and is provided my mechanosensory cells in the wall endothelium (mechanoreceptors). The mechanoreceptors can estimate the shear stress at the wall and pass the corresponding signal into the middle (smooth muscle) layer. Depending on the signal the muscle contracts or relaxes, influencing the lumen area and keeping $\tau_w = \text{const}$.

Optimal branching angles at bifurcations can also be provided in a growing body by the mechanoreceptors. As it had been observed by surgeons, when a blood vessel is cut at the bifurcation, the blood jet has the same angle with the axis of the main vessel as the dissected branch, so in an optimal case the branching angle corresponds to the jet flow and provides minimal shear stress at the wall at the bifurcation point (Fig. 8a). Let us suppose that the branching angle undergoes some perturbation due to a developmental problem (Fig. 8b,c). In that case the shear stress will be greater than the optimal value at the inner or outer side of the daughter vessels. Information on the non-homogeneous stress distribution will be transferred by the mechanoreceptors into the other layers of the blood vessels providing their non-uniform growth and consequent correction of the perturbed branching angles towards the optimal values.

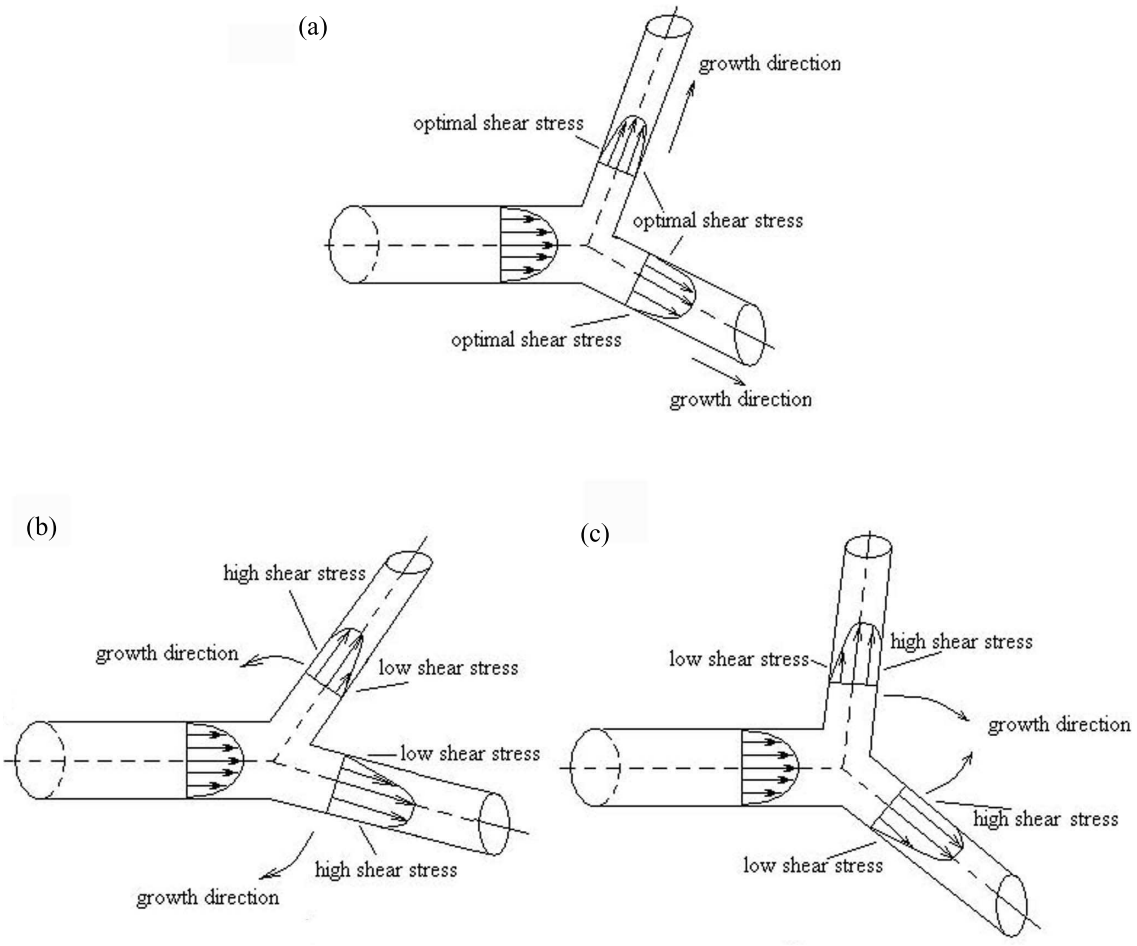

Fig. 8. Stress distribution in an arterial bifurcation at optimal (a), too small (b), and large (c) branching angles.

Simplicity of both the problem formulation and physiological explanation of the optimal blood vessel geometry and mechanism of its formation in a growing body attracts the attention of scientists to Murray's law. Some generalizations of the law have been proposed for the fluid flow in the distensible tubes [14], which is important for the realistic arterial systems, and for the flow of a non-Newtonian liquid with $\mu \sim d^{\alpha}$ in a rigid tube, which concerns the blood flows in small intraorgan arteries and for some other cases [37]. The results of averaged calculated values λ obtained from measurement data are summarized in Table 1.

For the coronary vasculature, which is accessible for the blood flow during the diastole when the heart is relaxed, a good agreement with Murray's law was also observed [101–104]. The distributing arteries are placed at the outer surface of the heart and possess the optimality parameter $\zeta = \left(d_1^3 + d_2^3\right)/d_0^3 = 0.991$ and the branching ratio $K = \left(d_1^2 + d_2^2\right)/d_0^2 = 1.129$; so the flow velocity decreases while the blood moves through a parent vessel into the daughter branches [104]. The delivering vessels deliver the blood into the cells; they are distributed inside the heart and possess $\zeta = 0.791$ and $K = 1.011$, so the blood velocity remains almost constant when the blood moves inside the heart tissues. The parameters of both subsystems correspond to the model of an optimal pipeline [4].

Relationship (12) has also been obtained in the detailed measurements on the fluid and gas transport systems in fish and insects, the trophic fluid transport systems of a variety of suspension-feeding marine invertebrates (molluscs, brachiopods, lophophorates, sponges) [44], the conducting systems of plant

Table 1. Power λ in Murray's law calculated on the measured data

Preparation	λ	Source
Small intestine of a dog	2.99	[49]
Lung arteries of a dog	2.61	[57]
Lung veins of a dog	2.76–3.01	
Human lung	2.91	[99]
Human aorta and large bronchial arteries	2.33	[92]
Coronary vasculatures of rats, monkeys, humans	2.45–3.02	[101–103]
Coronary arteries of a rat	2.86–3.14	[52]
Human pial arteries (in brain)	2.98	[41]
Coronary arteries of a pig	2.98	[93]
Human coronary arteries	3.02	[77]
Arteries of a chicken's embryo	2.99	[96]

leaves [29,30,53], tree branchings [105], and even in the bifurcations of axons [5]. In contrast to the arterial systems, the physiological mechanisms that can provide development of the optimal tree-like transportation networks in all the mentioned systems are not clear. For instance, in plants the conducting elements are lifeless conduits formed by the cell walls of the cells that had been destroyed at a certain stage of their development, so the corresponding direct regulation of the diameter of the conduit via the wall receptors is impossible.

5. A MODEL OF THE OPTIMAL SYMMETRIC BRANCHING PIPELINE

According to Murray's model the relationship $Q \sim d^3$ is a condition of optimality of a single tube. A model of an optimal binary tree (Fig. 9a), which provides liquid delivery at minimum total energy cost, was proposed in [4] and generalized to the m-branching pipeline (Fig. 9b) in [30]. Each tube of the pipeline is divided into m tubes with equal lengths and diameters, so the number of the tubes in the generation $j = 1...n$ is m^{j-1}, the total volume and resistivity of the pipeline are [30]:

$$\begin{aligned} V &= \sum_{n=0}^{N} \pi d_n^2 L_n m^n/4 = L_0 \sum_{n=0}^{N} m^{n/2} \varphi_n \pi d_n^2, \\ Z &= \frac{P_0 - P_{N+1}}{Q_0} = 8\pi\mu \sum_{n=0}^{N} r_n^{-\chi} L_n m^{-n} = \xi L_0 \sum_{n=1}^{N} m^{-3n/2} \varphi_n \left(\pi d_n^2\right)^{-\chi}, \\ \dot{W} &= (P_0 - P_{n+1})\, Q_0 = Q_0^2 \xi L_0 \sum_{n=1}^{N} m^{-3n/2} \varphi_n \left(\pi d_n^2\right)^{-\chi} = Q_0^2 Z, \end{aligned}$$

where Q_0 is the total volumetric rate, P_j are pressures in the nodes, $\varphi_j = L_j/\sqrt{S_j}$, μ is the fluid viscosity, S_j is the area of the influence domain (drainage area) of the j-th tube (Fig. 9b), $\chi = 1$ for the Darcy flow, and $\chi = 2$ for the Poiseuille flow.

The solution of the optimization problem $\dot{W} \to \min$ for the branching pipeline is [30]:

$$d_n = d_0 m^{\frac{-n}{\chi+1}} \quad or \quad d_{n+1} = d_n m^{\frac{-1}{\chi+1}}. \tag{14}$$

For a binary tree $m = 2$ and (14) gives $d_{n+1} = d_n/\sqrt[3]{2} \approx 0.8 d_n$. It is worth notion that the relation $d_{n+1} = 0.8 d_n$ was used in the very first model of the arterial tree proposed by Young in 1808 without explanations [100].

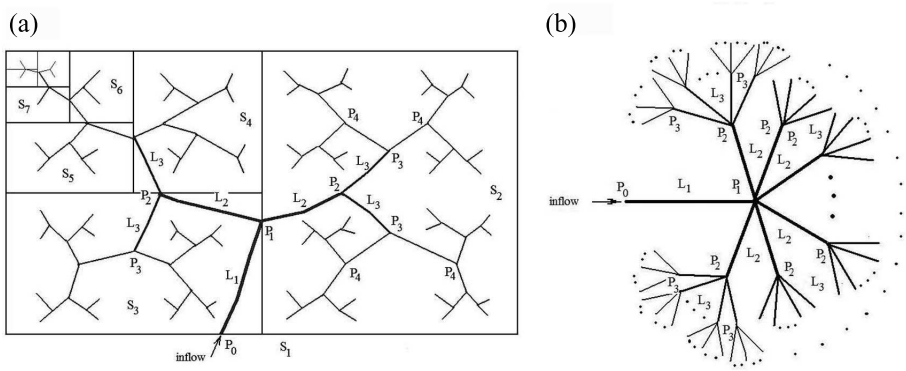

Fig. 9. Branching binary tree and the influence domains of the branches of different order (a) and *m*-branching tree-like system (b). Dots correspond to the tubes that have been omitted for clearness.

6. OPTIMAL BRANCHING PATTERNS IN PLANT VASCULATURES

The geometry of the plant leaf venation has been investigated on high-resolution digital pictures of fresh-cut leaves using developed image analysis software [33,35,39]. As the first step the leaf blade and the veins were detected using contrast analysis and recognition of the veins by a sliding matrix (Fig. 10, lower part of the leaf). Then the axes (middle lines) of the veins in a bifurcation were allocated and the corresponding diameters and branching angles were measured. Then the vein lengths L_i and the areas S_i of the leaf blade, which are supplied with sap through distinct veins (Fig. 10, upper part of the leaf) were measured. By using the developed software, some 1000 images of dicotyledonous leaves of different shape, size, and venation type have been investigated (200–250 bifurcations at each image).

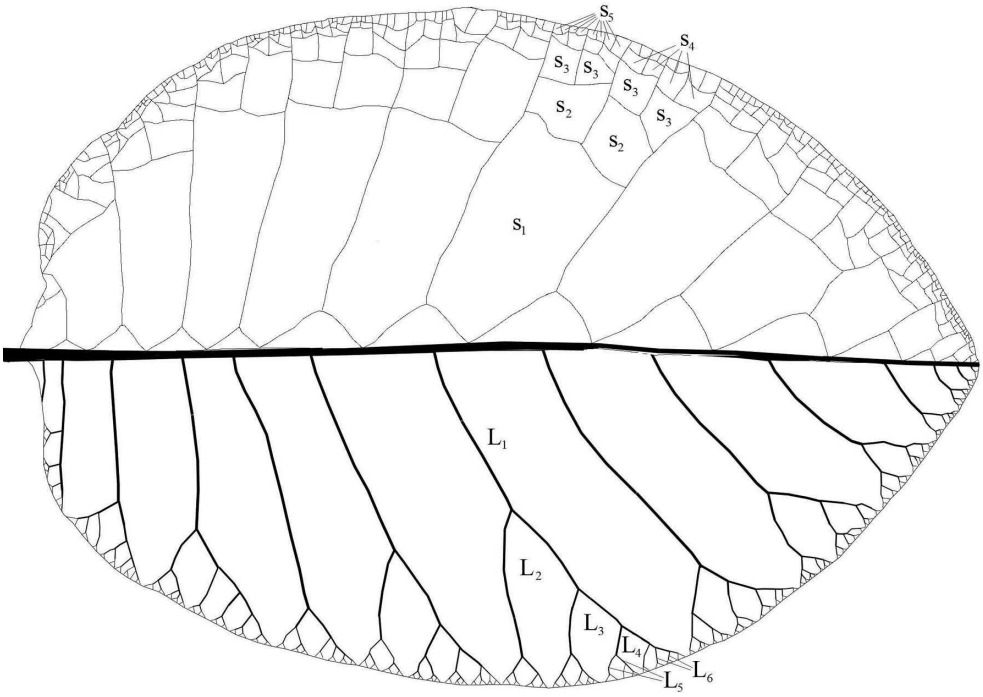

Fig. 10. *Cotinus obovatus* leaf with tree-like branching systems of veins (lower part of the leaf) and their influence domains (upper part of the leaf).

As it was revealed by measurements, Murray's law is also valid for bifurcations of the large veins. It is interesting to note that the correspondence to Murray's law with $\lambda = 3$ is better in leaf venations than in arterial bifurcations. Later the same result was obtained on the microscopic measurements of cut samples of vein bifurcations [53]. The dependence of the optimality parameter ζ_j on the diameter of the parent vein d_{j0} of the corresponding bifurcation is presented in Fig. 11a. Although the distribution patterns are distinct for different plant families, the subsystems of the distributing and delivering veins can be distinguished for each image in the same way as it was done for the arterial systems [103,104]. The distributing vessels exhibit optimal transport properties ($< \zeta >= 1 \pm 0.021$) at different diameters ($d_0 = 1$–5 mm) and provide the sap flow through the bifurcations at a relatively constant flow rate ($K \sim 1$). The delivering veins are characterized by some scatter in the optimality coefficient ($0.5 \leq \zeta \leq 2.5$) and the branching coefficient K, while the averaged value $< \zeta > \sim 1$ (Fig. 11a). The averaged value of the non-dimensional parameter $\chi = \cos(\alpha_{\text{opt}})/\cos(\alpha)$, which is a measure of the angle optimality, is $\langle \chi \rangle = 1 \pm 0.028$ ($\chi \in [0.772; 1.252]$), and the best correspondence of the branching angles to the optimal ones is observed for $K \in [1.2; 1.6]$, which corresponds to the majority of the small delivering veins.

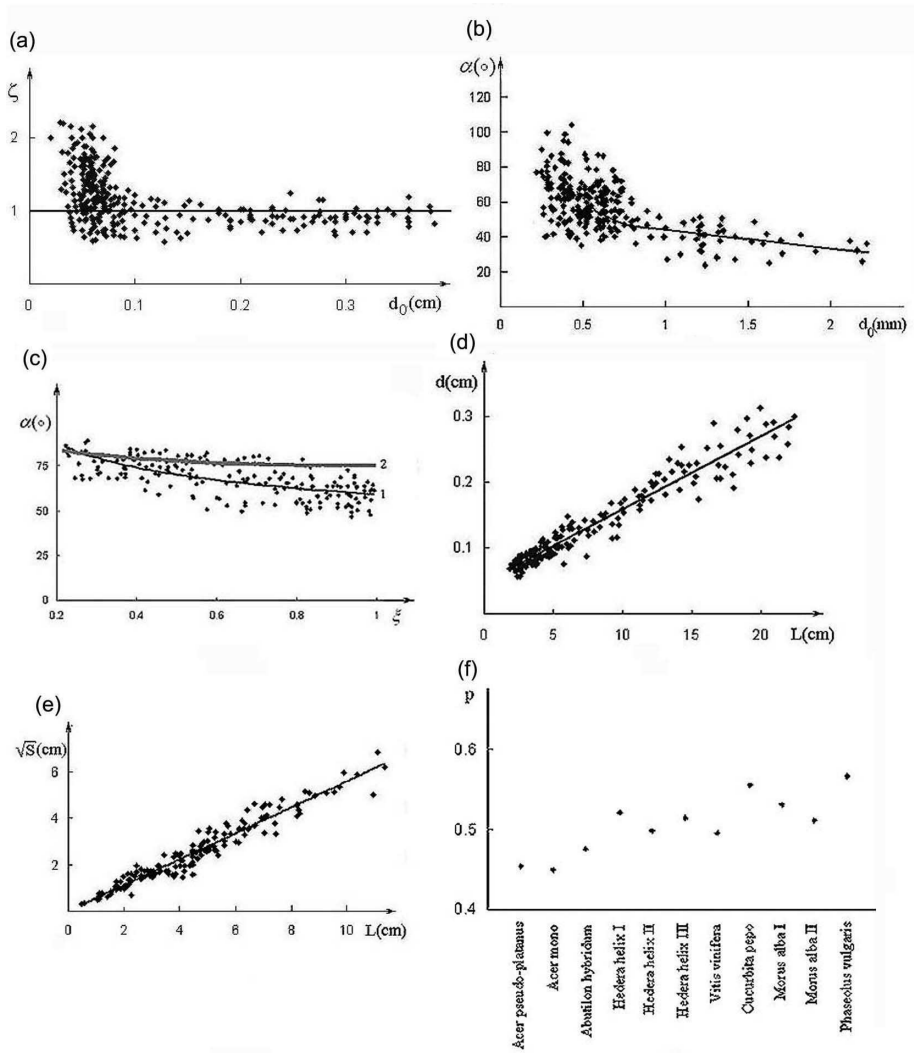

Fig. 11. Dependences $\zeta(d_0)$ (a), $\alpha(d_0)$ (b), $\alpha(\xi)$ (c), $L_j(d_j)$ (d), and $\sqrt{S_j}(L_j)$ (e) for the leaf venation, and the exponent p in the dependence $L \sim S^p$ (f) for some plant families.

The concept of distributing and delivering vessels was proposed in [103] and similar $\zeta(d_0)$ and $K(d_0)$ dependences were obtained for the brain arteries [50,55], coronary arteries [103,104], and other mammalian vasculatures. The Roux rules are also valid in the vein bifurcations: a larger daughter vessel has a smaller branching angle, the small veins of the last branching orders are almost perpendicular to the parent vessel, and the daughter vessels with equal diameters have almost equal branching angles.

The dependence of the branching angle on d_0 is similar to the dependence $\zeta(d_0)$, so the distributing veins have the total branching angle that is either constant or slightly decreases with d_0 (Fig. 11b). The branching angles exhibit some variations relative to the optimal values calculated from (1). The dependence $\alpha(\xi)$ is presented in Fig. 11b, where $\alpha = \alpha_1 + \alpha_2$ is the total branching angle, ξ is the asymmetry coefficient. Line 1 in Fig. 11c corresponds to the averaged values α at each ξ and line 2 corresponds to the optimal angle α calculated from (13). The divergence between the measurement data and optimal values is noticeable, which is in agreement with data obtained and calculated for the arterial bifurcations [102]. The numerical calculations of the costs of a small alteration in the branching angles of the arterial vessels revealed that the scatter in 10–15° corresponds to 5% energy loss relative to the optimal value, which is insignificant [102].

Perfect linear dependences between the length and diameter of the veins $L_j(d_j)$ (Fig. 11d) and the length of the vein and the area of its influence domain $\sqrt{S_j}(L_j)$ (Fig. 11e) can be observed for all the investigated leaf blades, which is a general and strict tendency in the construction of the conducting systems in the leaves. In other words, a longer vein supplies a larger area of the leaf blade. The scatter in the dependences $L_j(d_j)$ and $\sqrt{S_j}(L_j)$ is the smallest in comparison with other measured regularities. Since the geometry of the areas is distinct in different leaves (curvilinear triangles, quadrangles, hexagons, sectors of circle, etc.), geometric similarity cannot determine the observed dependences. The simplest explanation of the regularity may be given supposing the transport of water and dissolved substances is provided by the lateral surface Σ of the vein. For a circular cylinder $\Sigma \sim d \cdot L$ and taking into account the measured regularity $L \sim d$ we obtain $\Sigma \sim d^2$. For the steady flow through the tube the volumetric flow rate $Q \sim d^2$ and in that way $\Sigma \sim Q$. The most natural assumption is that the area of the influence domain is related to the flow rate because the area is formed by the cells that receive the necessary components and water from that vein. As it can be seen from Fig. 11f, the exponent in the dependence $L = aS^p$ is slightly bigger than 0.6, so the appropriate mathematical model is of great importance for the explanation of the obtained regularity because both dependences $L_j(d_j)$ and $L_j \sim S_j^p$ can not be explained by the theoretical concept (11) or its variation for the viscous steady flow in the rigid tube. The value a measured for a wide variety of plant families also belongs to a surprisingly narrow range $a = 0.317 \pm 0.022$, which points to the scale-independent character of the leaf conducting systems. As a similar dependence $L \sim S^p$ with $p = 0.5$–0.6 was obtained in a series of measurements on river basins (Hack's law) [15], we may conclude that general physical laws determine evolutionary optimization of the long-distance branching transport systems in the nature. The water flow in the river basins can move sand and soil along the bed producing variations of the bottom roughness, flow direction, and local velocity [21]. Because the water flow is determined by the gravity and hydrodynamic laws at a given landscape, the resulting landscape transformations lead the river system towards the state with minimal total energy dissipation [13,81,84]. The problem of statistical similarity between the geometrical structure of the leaf veins and riser systems is intensively discussed in the literature [63,87].

7. MODEL OF AN OPTIMAL PIPELINE WITH PERMEABLE WALLS

As is was shown by direct experimental measurements of the pressure–flow relationships in separate vessels, veins, and vein systems, the hydraulic conductivity of the plant conducting pathways is described by Poiseuille's law $\delta P = QZ$, where $Z = aZ_p$, Z_p is the Poiseuille resistivity, $a = \text{const} > 1$ [9,11]. A model of the plant venation as a branching system of rigid tubes with permeable walls was proposed in [34,37]. The axisymmetric flow $\vec{v} = (v_r, 0, v_x)$ of a viscous liquid along the tube driven by the pressure drop $\delta p = p_1 - p_2 > 0$ was considered and both the passive outflow through the penetrable wall due to the pressure drop $p - p*$, $p* = \text{const}$ (Fig. 12) and an active pressure-independent transport due to the cellular mechanisms were taken into account.

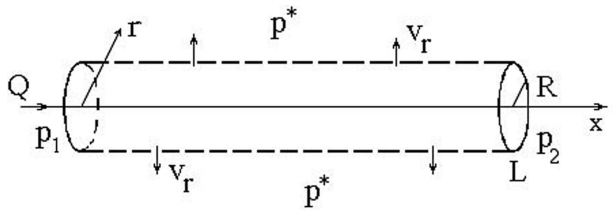

Fig. 12. A model of the leaf vein.

The governing equations for an incompressible flow at $Re << 1$ in the long tube ($R/L << 1$) are Stokes's equations [69]:

$$\frac{1}{r}\frac{\partial}{\partial r}(rv_r)+\frac{\partial v_x}{\partial x}=0,\ \ \frac{\mathrm{d}p}{\mathrm{d}x}=\mu\left(\frac{\partial^2 v_x}{\partial r^2}+\frac{1}{r}\frac{\partial v_x}{\partial r}\right) \tag{15}$$

with the boundary conditions

$$\begin{aligned} &p|_{x=0}=p_1,\, p|_{x=L}=p_2,\, v_x|_{r=R}=0,\, \left.\frac{\partial v_x}{\partial r}\right|_{r=0}=0,\\ &v_r|_{r=0}=0,\, v_r|_{r=R}=w(x)+k(p(x)-p^*), \end{aligned} \tag{16}$$

where $p(x)$ is the pressure inside the tube, k is the wall permeability, μ is fluid viscosity, $w(x)$ is an active component of the outflow through the wall.

The solution of problem (15)–(16) for an arbitrary $w(x)$ is

$$\begin{aligned} p(x) &= p^*+\delta_1 ch(\nu x)+\frac{\nu 2k}{\zeta}(x,\nu)+Bsh(\nu x),\\ V_r(r,x) &= \frac{\nu^2}{16\mu}\left(2R^2r-r^3\right)\left(\delta_1 ch(\nu x)+Bsh(\nu x)+\frac{\nu}{2k}\zeta(x,\nu)+\frac{w(x)}{k}\right), \\ V_x(r,x) &= \frac{\nu}{4\mu}\left(r^2-R^2\right)\left(\delta_1 sh(\nu x)+Bch(\nu x)+\frac{1}{2k}\zeta_x^{/}(x,\nu)\right), \end{aligned} \tag{17}$$

where $\nu=\sqrt{16k\mu/R^3}$, $\zeta(x,\nu)=e^{\nu x}\int\limits_0^x e^{-\nu x}w(\varsigma)\,\mathrm{d}\varsigma-e^{-\nu x}\int\limits_0^x e^{\nu x}w(\varsigma)\,\mathrm{d}\varsigma$,

$B=\left(\delta_2-\frac{\nu}{2k}\zeta(L,\nu)\right)(sh(\nu L))^{-1}-\delta_1 cth(\nu L)$, $\delta_1=p_1-p^*$, $\delta_2=p_2-p^*$.

Basing on statistical data [17,63], numerical calculations on (16) were made for some simplified functions $w(x)$ [37]:

$$\begin{aligned} &I.\ \ w(x)=w^*=\mathrm{const}>0,\\ &II.\ \ w(x)=a(1-x/L),\\ &III.\ \ w(x)=be^{-cx}, \end{aligned} \tag{18}$$

where a, b, and c are given constants, calculated in order to provide the same total active outflow $\Phi=2\pi R\int_0^L v_r(R,x)\,\mathrm{d}x$ through the wall providing a possibility of the comparative study of the three different functions (18).

For the case when all the liquid flowing along the tube is transported through the wall into the plant cells so $p(L)=p*$ and $Q=\Phi$, a concept of the optimal tube can be proposed. Then the hydraulic resistance of the tube is

$$Z = Z_p\Psi, \Psi = \frac{th(\nu L)}{\nu L} - \frac{\zeta(L)}{2\nu L^2\left(k\delta_1\frac{sh(\nu L)}{\nu L} + \frac{1}{L}\int\limits_0^L w(x)\,ch(\nu(x-L))\,dx\right)} \tag{19}$$

and for the cases *I–III* the following results are obtained [37]:

$$\begin{aligned} &I.\ \Psi^{(1)} = \frac{th(l)}{l} - \frac{F(l)}{1+\chi^{(1)}},\\ &II.\ \Psi^{(2)} = \frac{th(l)}{l} - \frac{1-sh(l)}{\left(1-ch(l)+lsh(l)\left(1+\chi^{(2)}\right)\right)l},\\ &III.\ \Psi^{(3)} = \frac{th(l)}{l} - \frac{\left(1-\eta^2\right)(ch(l)-1)e^{-l\eta}}{\chi^{(3)}lsh(l)(1-\eta^2)+\eta le^{-l\eta}(sh(l)+lch(l))}, \end{aligned} \tag{20}$$

where $l = \nu L$, $\eta = c/\nu$, $F(x) = (ch(x)-1)/(x\cdot sh(x))$, $\chi = k\delta_1/w(0)$ is a ratio of the velocities of the passive and active transport at the inlet and $\chi^{(1)} = k\delta_1/w^*$, $\chi^{(2)} = \chi^{(1)}a^\circ$, $\chi^{(3)} = \chi^{(1)}b^\circ$.

The dependences were investigated in depth by numerical computations within a wide range of the values of all the model parameters and the relationships between the active and passive outflow are discussed in [37]. The values of the viscous dissipation

$$\Theta = 2\pi\int\limits_0^L dx\int\limits_0^R \tau_{ik}v_{ik}r\,dr, \tag{21}$$

where v_{ik} and $\tau_{ik} = 2\mu v_{ik}$ are the strain rate, and shear stress tensors are calculated for the limit cases of the pure active ($\chi = 0$) and passive ($\chi = \infty$) transport in the following forms:

$$\begin{aligned} &I.\ \Theta^{(1)} = \Theta^P\left(1-\varepsilon+\frac{1}{3}\varepsilon^2\right),\\ &II.\ \Theta^{(2)} = \Theta^P\left(1-\frac{4}{3}\varepsilon+\frac{8}{15}\varepsilon^2\right),\\ &III.\ \Theta^{(3)} = \Theta^P\left(1+\frac{2}{1+\eta^2}\left(\varepsilon-\eta\varepsilon^2\right)\right) \end{aligned} \tag{22}$$

for $\chi = 0$ and

$$\Theta^{(0)} = \Theta^P\left(\frac{1}{2}\left(1+ch(l)\frac{sh(l)}{l}\right) - (\varepsilon-1+ch(l))\frac{sh(l)}{l} + (\varepsilon-1+ch(l))^2\frac{ch(l)\cdot sh(l)-l}{2lsh^2(l)}\right) \tag{23}$$

for $\chi = \infty$,
where $\Theta^P = 8\mu LQ^2/(\pi R^4)$ is the dissipation in the Poiseuille flow through the tube with an impermeable wall, $\varepsilon = \Phi/Q$ is the ratio between the outflow through the wall and the inflow at the tube inlet. When $Q = \Phi$, (22)–(23) gives the following values

$$\begin{aligned} \Theta^{(1)} &= \Theta^P/3,\\ \Theta^{(2)} &= \Theta^P/5,\\ \Theta^{(3)} &= \Theta^P(3-2\eta+\eta^2)/(1+\eta^2),\\ \Theta^{(0)} &= \Theta^P(ch(l)sh(l)-l)/(2lsh^2(l)), \end{aligned}$$

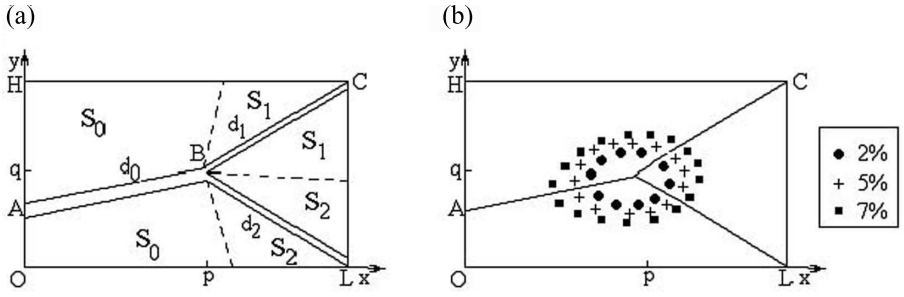

Fig. 13. Structure of the bifurcation in a rectangular microcirculatory cell (a) and deviations of the total energy cost of small variations in the position of the bifurcation point B (b).

which differ from Θ^P by a constant (for $\Theta^{(1)}$ and $\Theta^{(2)}$), by a geometry-independent term (for $\Theta^{(3)}$), or by a term that in the case of the sap flow in the leaf veins ($\mid l \mid \leq 0.5$) gives $\Theta^{(0)} = \Theta^P(1/3 + o(l^2))$, so the solution of the optimization problem (11) for a single tube gives the same relationship $Q \sim d^3$ that had been obtained for the Poiseuille flow in the tube with the impermeable wall.

The same optimization problem (11) has been solved in the application to a single bifurcation (Fig. 7a) of the tubes with permeable walls in the form:

$$\dot{W} = \sum_{j=0}^{2} (Q_j (Z^{(j)})^2 + \chi \pi R_j^2 L_j) \rightarrow \min. \tag{24}$$

As it was shown by numerical calculations, the minimal total energy expense is reached when the relationships (9)–(10) between the diameters and branching angles are valid. Any small variation of the position (p, q) of the bifurcation point B leads to variations of the branching angles within the experimentally observed limits $\delta\alpha \sim 10$–25° and insignificant changes in the value $\dot{W}$ ($\pm$5–7%) in comparison with the optimal case (Fig. 13) [33]. In that way the cost of a development mistake is relatively small and the mistake may be corrected at the consequent branchings by corresponding variations of their angles providing balance between the fluid outflow through the wall of the conducting system and its consumption by the cells in the corresponding influence domain.

A fruitful development of the proposed theory is connected with the modelling of the plant leaf as a set of interconnected microcirculatory cells separated by main veins and their branchings [31,40]. A similar model of blood circulation in the muscles was proposed in [70] without taking into consideration osmotic factors.

8. CONCLUSIONS

A simple model of the fluid flow in the plant conducting element as in a tube with permeable walls has been used purposely to obtain an analytical solution of the optimization problem as it was done by Murray. Many important factors like osmotic pressure, interconnection between the conducting element and the leaf mesophyll via apoplast and symplast transport, water evaporation, and other physical phenomena are not taken into account in this model. In the same way Murray's model of the steady flow in the rigid tube is unrealistic for the description of the blood flow in arteries, which is in fact pulsatile. Certainly, more complicated problems can be formulated for the pulsatile flow through the distensible tube as well as for the long-range transport of water and dissolved components including both hydrodynamic and osmotic factors. The solutions of the corresponding optimization problems can be obtained by numerical computations, so the power law $Q \sim d^\lambda$ can be refined. As it was shown in the present paper, at some assumptions the solution of the optimization problem for the tubes with permeable and impermeable walls lead to the same dependence $Q \sim d^3$. It is very likely that the corresponding solutions for the fluid flow in the trophic systems

of sponges and intracellular liquid flow along the axon in the nerve cells will also give similar solutions with $\lambda \sim 3$. It is known that some optimal relations are implemented by the nature in various constructions and at different levels from the intracellular level to the entire organisms. Arrangement of the fibres in the biocomposites, leaves in the tree crowns, flowers in blossoms, and proportions of the bodies are tightly connected with the Golden section and the Fibonacci numbers. When the Golden section is used as the proportion between the subparts of the system, one can expect maximal strength and durability of the entire construction at both micro- and macrolevels, because the Golden section is the solution of the mechanical optimization problem. When the leaves in plants, flowers, and seeds in the blossom clusters are disposed in two families of spirals and the number of the spirals is presented by two of the Fibonacci series, the total overlap area of the leaves is minimal, so the leaves receive maximal sun radiation, and the empty space between the seeds or flowers in the blossom is minimal, which corresponds to the optimal solution of the packing problem. The location of the tree branches corresponds to the maximal effective leaf area for light absorption and photosynthesis [20]. The honeycomb is an optimal geometrical solution for maximizing the total area at a given amount of material for the walls.

A long list of examples of optimal constructions in the living nature can be given and a problem that is widely discussed in the literature is at which level the optimal solution is provided. As one can see, mechanical factors can provide development of optimal transportation systems in the growing organs and organisms. For instance, the mechanosensory cells in the blood vessels can estimate the shear stress at the wall and control the vessel lumen and growth anisotropy, providing development of both optimal vessel with $Q \sim d^3$ and optimal branching angles $\alpha_{1,2}(d_0, d_1, d_2)$ keeping $\tau_w = \text{const}$. In the venations of the plant leaves the natural explanation of the optimal relationships between the diameters of the branches at a bifurcation (Murray's law) and the length of the vein and the area S of its influence domain (Hack's law) can be given basing on the mechanical factors only. As it follows from the solution of the optimization problem for a single tube with permeable walls, at some assumptions ($\Phi \sim Q, \Phi << Q$ and some others) the total energy cost of the viscous flow is minimal when $Q \sim d^3$. If $\Phi \sim S$ in each conducting element, there is a balance between the inflow of the liquid in the conducting element and its consumption by live cells in the influence domain. The balance between the liquid inflow and consumption in each microcirculatory cell of a leaf can be considered as a possible mechanism of optimal transport systems formation in plants. For instance, let a mistake in the position of B be reached and the branching angles (or one of them) be less than its optimal value (as it is presented in Fig. 8b). In this case the area of the region BCL will be less than the optimal one and the living cells located in BCL will obtain more water and nutrients and will grow faster than the cells in the areas ABCH and ABLO, which will experience some insufficiency, because their total area will be too large. The increased growth of the region BCL and decreased growth of the regions ABCH and ABLO will result in increasing the branching angle CBL up to the optimal value when the total supply of water and nutrients through the porous walls of every conducting element will be balanced with consumption by the cells located in the corresponding regions.

Genetic mechanisms of the development of optimal bifurcations in the conducting systems of plants and animals are also discussed in the literature [56]. The importance of the genetic factors can be directly observed in the incorrect structure of the conducting pathways in some genetically modified plants. Moreover, mechanical and genetic factors are interconnected in both embryonic development and future growth of the organism and its adaptation to the given environmental conditions, including the static and dynamic loads, which can change the processes at the cellular level including cell divisions and synthesis of proteins [88]. The problems of design principles and mechanisms of the formation of optimal structures and systems in biological cells, tissues, and organisms are important as a possibility of using the nature-inspired optimal solutions for technical and biomedical applications.

ACKNOWLEDGEMENTS

I deeply thank professors D. Jou, W. Muschik, V. Cimmelli, J. Verhás, and P. Ván for stimulating and helpful discussions on the topic.

Natalya N. Kizilova received her PhD in Mechanics of Fluids, Gas, and Plasma from Kharkov National University in 1993. Currently Associate Professor Kizilova is Head of the Department of Theoretical Mechanics of Kharkov National University, Ukraine. Her main research fields are wave propagation in fluid-filled elastic tubes and complex systems of tubes; wave propagation and dispersion in saturated porous media; modelling the circulatory system; pulse wave analysis; long-distance transport networks; optimal transport systems in the nature; multicriteria and evolutionary optimization; modelling growing biological continuous media. She has published numerous research papers in English as well as in Russian.

REFERENCES

1. Anisimov, A. V. and Ratkevich, S. *Transport of Water in Plants. Investigation by Impulse NMR Method*. Nauka, Moscow, 1992 (in Russian).
2. Aumann, C. A. and Ford, D. E. Modeling tree water flow as an unsaturated flow through a porous medium. *J. Theor. Biol.*, 2002, **219**, 415–429.
3. Canny, M. J. Embolisms and refilling in the maize leaf lamina, and the role of the protoxylem lacuna. *Am. J. Bot.*, 2001, **88**, 47–51.
4. Chernousko, F. L. Optimal structure of branching pipelines. *Prikl. Matem. Mech.*, 1977, **41**, 376–383 (in Russian).
5. Chklovskii, D. B. and Stepanyants, A. Power-law for axon diameters at branch point. *BMC Neurosci.*, 2003, **4**, 18–25.
6. Dixon, H. H. *Transpiration and the Ascent of Sap in Plants.* Macmillan and Co., London, 1914.
7. Dixon, H. H. and Joly, J. On the ascent of sap. *Phylos. Trans. R. Soc. London, B*, 1895, **186**, 563–576.
8. Edwards, E. J. Correlated evolution of stem and leaf hydraulic traits in *Pereskia* (Cactaceae). *New Phytol.*, 2006, **172**, 479–489.
9. Ellerby, D. J. and Ennos, A. R. Resistances to fluid flow of model xylem vessels with simple and scalariform perforation plates. *J. Exp. Bot.*, 1998. **49**, 979–985.
10. Esau, K. *Anatomy of Seed Plants*. 2nd edn. John Wiley & Sons, 1977.
11. Ewers, F. W., Fisher, J. B. and Chiu, Sh.-T. Water transport in the liana *Bauhinia fassoglensis* (Fabaceae). *Plant Physiol.*, 1989, **91**, 1625–1631.
12. Gary, Ch., Le Bot, J., Frossard, J.-S. and Andriolo, J. L. Ontogenic changes in the construction cost of leaves, stems, fruits, and roots of tomato plants. *J. Exp. Bot.*, 1998, **49**, 59–68.
13. Giacometti, A. Local minimal energy landscapes in river networks. *Phys. Rev. Ser. E*, 2000, **62**, 6042–6051.
14. Grygoryan, S. S. and Gotsyridze, N. Sh. Optimal organization of branching vascular network at pulsatile flow. In *Mechanics of Biological Continuous Media*. Moscow University Press, Moscow, 1986, 125–131.
15. Hack, J. T. Studies of longitudinal profiles in Virginia and Maryland. *US Geol. Surv. Prof. Pap*., 1957.
16. Henton, S. M., Greaves, A. J., Piller, G. J. and Minichin, P. E. H. Revisiting the Münch pressureflow hypothesis for long-distance transport of carbohydrates: Modelling the dynamics of solute transport inside a semipermeable tube. *J. Exp. Bot.*, 2002, **53**, 1411–1419.
17. Hickey, L. J. Classification of the architecture of dycotyledonous leaves. *Am. J. Bot.*, 1973, **60**, 17–33.
18. Holbrook, N. M., Ahrens, E. T., Burns, M. J. and Zwieniecki, M. A. In vivo observation of cavitation and embolism repair using magnetic resonance imaging. *Plant. Physiol.*, 2001, **126**, 27–31.
19. Hölttä, T. H., Vesala, W. T., Perämäki, M. and Nikimaa, E. Relationships between embolism, stem water tension, and diameter changes. *J. Theor. Biol.*, 2002, **215**, 23–38.
20. Honda, H. and Fisher, J. B. Tree branch angle: Maximizing effective leaf area. *Science*, 1978, **1999**, 888–889.
21. Horton, R. E. Erosional development of streams and their drainage basins; hydrophysical approach to quantitative geomorphology. *Bull. Geol. Soc. Am.*, 1945, **56**, 275–370.
22. Huang, W., Yen, R. T., McLaurine, M. and Bledsoe, G. Morphometry of the human pulmonary vasculature. *J. Appl. Physiol.*, 1996, **81**, 2123–2133.
23. Kargol, M. Osmotic, hydromechanic and energetic properties of modified Münch's model. *Gen. Physiol. Biophys.*, 1994, **13**, 3–19.
24. Kargol, M., Kosztolowicz, T., Markovski, A. and Przestalski, S. Energetic aspects of water transport across the plant root. *Acta Physiol. Plant.*, 1995, **17**, 327–332.

25. Kargol, M., Suchanek, G., Przestalski, S. and Kargol, A. Modification of integration system of long-distance transport of water in plants. Where the plant has its heart? *Cur. Topics Biophys.*, 2003, **27**, 3–9.
26. Karmanov, V. G., Lialin, O. O., Mamulashvili, G. G. et al. Water exchange dynamics of high plants and its informational role. *Physiol. Biochim. Vysshikh Rastenij*, 1974, **6**, 69–75 (in Russian).
27. Karmanov, V. G. and Meleshchenko, S. N. Mechanism of auto-oscillations of water metabolism in plants. *Biofizika*, 1982, **27**, 144–149 (in Russian).
28. Kedem, O. and Katchalsky, A. Thermodynamic analysis of the permeability of biological membranes to non-electrolytes. *Biochim. Biophys. Acta*, 1958, **27**, 229–246.
29. Kizilova, N. N. Computational approach to optimal transport network construction in biomechanics. *Lecture Notes Comp. Sci.*, 2004, **3044**, 476–485.
30. Kizilova, N. N. Construction principles and control over transport systems organization in biological tissues. In *Physics and Control* (Fradkov, A. L. and Churilov, A. N., eds). IEEE Computer Society, Washington, 2003, Vol. 1, 303–308.
31. Kizilova, N. N. Hydraulic properties of branching pipelines with permeable walls. *Int. J. Fluid Mech. Res.*, 2005, **32**, 98–109.
32. Kizilova, N. N. Liquid filtration in a microcirculatory cell of the plant leaf: A lumped parameter model. *Int. J. Fluid Mech. Res.*, 2007, **34**, 572–588.
33. Kizilova, N. N. Motion of water and solvents in plant leaves: Interrelation of hydromechanical and osmotic factors. In *Liquid Matter Conference. Book of Abstracts*. Utreht, 2005, 74.
34. Kizilova, N. Optimal long-distance transport systems in nature: Control and applications. In *International Congress on Industrial and Applied Mathematics. Abstract Book*, 2007, 286–287.
35. Kizilova, N. N. Optimization of branching pipelines on basis of design principles in Nature. In *Proceedings of the European Congress on Computational Methods in Applied Sciences*. Finland, 2004, Vol. 1, 317–328.
36. Kizilova, N. N. Thermodynamic model of heat and mass transfer and motion of liquids in plant leaves. In *2-nd International conference "Physics of liquid matter: modern problems", Book of Abstracts*, 2003, 173.
37. Kizilova, N. N. and Popova, N. A. Criterions of optimum performance of branching transport system of alive nature. *Kharkov National University Vestnik. Ser. Matem., Priklad. Matem., Mekh.*, 1999, **444**, 148–156.
38. Kizilova, N. N. and Popova, N. A. Investigation of transport systems of leaves. *Probl. Bion.*, 1999, **51**, 71–79 (in Russian).
39. Kizilova, N. N. and Posdniak, L. O. Biophysical mechanisms of long-distance transport of liquids and signaling in high plants. *Biophys. Bull.*, 2005, **15**, 99–103.
40. Kizilova, N. N. and Stolkiner, M. G. Investigation of liquid transport and the structure of optimal microcirculatory cell. *Probl. Bion.*, 2002, **57**, 103–108.
41. Kobari, M., Gotoh, F., Fukuuchi, Y., Tanaka, K., Suzuki, N. and Uematsu, D. Blood flow velocity in the pial arteries of cats, with particular reference to the vessel diameter. *J. Cereb. Blood Flow Metab.*, 1984, **4**, 110–114.
42. Kursanov, A. L. *Transport of Assimilates in Plants*. Nauka, Moscow, 1976 (in Russian).
43. Kushnirenko, M. D., Pecherskaya, S. N., Bashtovaya, S. I. et al. Influence of chemical substances on kinetics of water exchange in leaves. *Biofizika*, 1991, **317**, 509–511 (in Russian).
44. La Barbera, M. Principles of design of fluid transport systems in zoology. *Science*, 1990, **249**, 992–1000.
45. Lampinen, M. J. and Noponen, T. Thermodynamic analysis of the interaction of the xylem water and phloem sugar solution and its significance for the cohesion theory. *J. Theor. Biol.*, 2003, **224**, 285–298.
46. Lazareva, N. P., Borisova, T. A. and Zolkevitch, V. N. On auto-oscillating character of pumping action of *Zea mays* L. root system. *Izv. AN SSSR*, 1986, 761–764 (in Russian).
47. Lighthill, M. J. Physiological fluid dynamics: A survey. *J. Fluid Mech.*, 1972, **52**, 475–497.
48. Linton, M. J. and Nobel, P. S. Loss of water transport capacity due to xylem cavitation in roots of two cam succulents. *Am. J. Bot.*, 1999, **86**, 1538–1543.
49. Mall, F. P. Die Blut und Lymphwege in Dunndarm des Hundes. Abhandlungen der mathematisch-physischen Classe der koniglich Sachsischen. *Ges. Wissensch.*, 1888, **14**, 151–200.
50. Mamisashvili, V. A. and Babunashvili, M. K. Criterium of optimal function of the systems of large and small pial apteries. *Fiziol. Zh. SSSR*, 1975, **61**, 1501–1506 (in Russian).
51. Martre, P., Cochard, H. and Durand, J. L. Hydraulic architecture and water flow in growing grass tillers (*Festuca arundinacea* Schreb.). *Plant Cell Environ.*, 2001, **24**, 65–76.
52. Mayrovitz, H. N. and Roy, J. Microvascular blood flow: Evidence indicating a cubic dependence on arteriolar diameter. *Am. J. Physiol.*, 1983, **245**, 1031–1038.
53. McCulloh, K. A., Sperry, J. S. and Adler, F. R. Water transport in plants obeys Murray's law. *Nature*, 2003, **421**, 939–942.
54. Meinzer, F. C., Woodruff, D. R., Domec, J.-Ch. et al. Coordination of leaf and stem water transport properties in tropical forest trees. *Oecologia*, 2008, **156**, 31–41.
55. Melkumjanz, A. M. Optimal structure of arterial network of muscles. *Bull. Exp. Biol. Med.*, 1978, **9**, 259–262.
56. Metzger, M. G. and Krasnov, M. A. Genetic control of branching morphogenesis. *Science*, 1999, **284**, 1635–1639.
57. Miller, W. S. The structure of the lung. *J. Morphol.*, 1893, **8**, 165–188.
58. Münch, E. *Stoffbewegungen in der Pflanze*. Verlag Gustav Fisher, Jena, 1930.

59. Murray, C. D. The physiological principle of minimum work. I. The vascular system and the cost of blood volume. *Proc. Natl. Acad. Sci. USA*, 1926, **12**, 207–214.
60. Murray, C. D. The physiological principle of minimum work applied to the angle of branching of arteries. *J. Gen. Physiol.*, 1926, **9**, 835–841.
61. Nardini, A., Salleo, S. and Raimondo, F. Changes in leaf hydraulic conductance correlate with leaf vein embolism in *Cercis siliquastrum* L. *Trees*, 2003, **17**, 529–534.
62. Pachepsky, L. B., Ferreyra, R. A., Collino, D. and Acock, B. Transpiration rates and leaf boundary layer parameters for peanut analyzed with the two-dimensional model 2DLEAF. *Biotronics*, 1999, **28**, 1–28.
63. Pelletier, J. D. and Turcotte, D. L. Shapes of river networks and leaves: Are they statistically similar? *Philos. Trans. R. Soc. Lond. Ser. B*, 2000, **355**, 307–311.
64. Polevoj, V. V. *Plant Physiology*. Vysshaya Shkola, Moscow, 1989.
65. Poluektov, R. A., Kumakov, V. A. and Vasylenko, G. V. Modeling of transpiration of agricultural plants. *Plant Physiol.*, 1997, **44**, 68–73.
66. Pries, A. R., Secomb, T. W. and Gaehtgens, P. Design principles of vascular beds. *Circ. Res.*, 1995, **77**, 1017–1023.
67. Rand, R. H. Fluid mechanics of green plants. *Ann. Rev. Fluid Mech.*, 1983, **15**, 39–45.
68. Rashevsky, N. Models and mathematical principles in biology. In *Theoretical and Mathematical Biology*. Mir, Moscow, 1968, 48–66.
69. Regirer, S. A. On the approximate theory of motion of a viscous incompressible fluid in the tubes with permeable walls. *Zh. Tekhn. Fiz.*, 1960, **30**, 639–643 (in Russian).
70. Regirer, S. A. and Shadrina, N. H. Blood flow in a capillary cell of muscle: 2d effects. *Izv. AN SSSR, Ser. MZG*, 1989, **5**, 94–100 (in Russian).
71. Rosen, R. *Optimality Principles in Biology*. Plenum Press, New York, 1967.
72. Sack, L, Streeter, Ch. M. and Holbrook, N. M. Hydraulic analysis of water flow through leaves of sugar maple and red oak. *Plant Physiol.*, 2004, **134**, 1824–1833.
73. Sack, L., Tyree, M. T. and Holbrook, N. M. Leaf hydraulic architecture correlates with regeneration irradiance in tropical rainforest trees. *New Phytol.*, 2005, **167**, 403–413.
74. Sack, L. and Frole, K. Leaf structural diversity is related to hydraulic capacity in tropical rain forest trees. *Ecology*, 2006, **87**, 483–491.
75. Sack, L. and Holbrook, N. M. Leaf hydraulics. *Annu. Rev. Plant Biol.*, 2006, **57**, 361–381.
76. Scholander, P. F., Hammel, H. T. and Hemmingsen, E. A. Sap pressure in vascular plant. *Science*, 1965, **148**, 339–346.
77. Schreiner, W., Neumann, F., Neumann, M., End, A. and Müller, M. R. Structural quantification and bifurcation symmetry in arterial tree models generated by constrained constructive optimization. *J. Theor. Biol.*, 1996, **180**, 161–174.
78. Schulte, P. J. Water flow through a 20-pore perforation plate in vessels of *Liquidambar styraciflua*. *J. Exp. Bot.*, 1999, **50**, 1179–1187.
79. Schulte, P. J. and Brooks, J. R. Branch junctions and the flow of water through xylem in Douglas-fir and ponderosa pine stems. *J. Exp. Bot.*, 2003, **54**, 1597–1605.
80. Shoshenko, K. A., Golub, A. S., Brod, V. I. et al. *Architectonics of the Blood Vasculatures*. Nauka, Novosibirsk, 1982 (in Russian).
81. Sinclair, K. and Ball, R. C. Mechanism for global optimization of river networks from local erosion rules. *Phys. Rev. Lett.*, 1996, **76**, 3360–3363.
82. Sleicher, R. O. *The Plant Water Regime*. Mir, Moscow, 1970 (in Russian).
83. Smith, A. M. Xylem transport and negative pressures sustainable by water. *Ann. Bot.*, 1994, **74**, 647–651.
84. Sun, T., Meakin, P. and Jossang, T. Minimum energy dissipation river networks with fractal boundaries. *Phys. Rev. Ser. E*, 1995, **51**, 5353–5359.
85. Thompson, M. V. and Holbrook, N. M. Scaling phloem transport: Water potential equilibrium and osmoregulatory flow. *Plant Cell Environ.*, 2003, **26**, 1561–1577.
86. Thompson, M. V. Scaling phloem transport: Elasticity and pressure–concentration waves. *J. Theor. Biol.*, 2005, **236**, 229–241.
87. Turcotte, D. L., Pelletier, J. D. and Newman, W. I. Networks with side branching in biology. *J. Theor. Biol.*, 1998, **193**, 577–592.
88. Turgeon, R. and Webb, J. A. Growth inhibition by mechanical stress. *Science*, 1971, **174**, 961–962.
89. Tyree, M. T. and Dixon, M. A. Cavitation events in *Thuja occidentalis*: Ultrasonic acoustic emissions from the sapwood can be measured. *Plant Physiol.*, 1983, **72**, 1094–1099.
90. Tyree, M. T. and Sperry, J. S. Vulnerability of xylem to cavitation and embolism. *Annu. Rev. Plant Physiol. Mol. Biol.*, 1989, **40**, 19–38.
91. Tyree, M. T. The Cohesion-tension theory of sap ascent: Current controversies. *J. Exp. Bot.*, 1997, **48**, 1753–1765.
92. Uylings, H. B. M. Optimization of diameters and bifurcation angles in lung and vascular tree structures. *Bull. Math. Biol.*, 1977, **39**, 509–519.
93. van Bavel, E. and Spaan, J. A. E. Branching patterns in the porcine coronary arterial tree. Estimation of flow heterogeneity. *Circ. Res.*, 1992, **71**, 1200–1212.

94. van den Honert, T. H. Water transport in plants as a catenary process. *Discuss. Faraday Soc.*, 1948, **3**, 146–153.
95. Vesala, W. T., Hölttä, T. H., Perämäki, M. and Nikimaa, E. Refilling of a hydraulically isolated embolized xylem vessel: Model calculations. *Ann. Bot.*, 2003, **91**, 419–428.
96. Vico, P. G., Kyriacos, S., Heymans, O., Louryan, S. and Cartilier, L. Dynamic study of the extraembryonic vascular network of the chick embryo by fractal analysis. *J. Theor. Biol.*, 1998, **195**, 525–532.
97. Wagner, O. E. Anisotropy of wave velocities in plants: Gravitropism. *Physiol. Chem. Phys. Med. NMR*, 1996, **28**, 173–186.
98. Westgate, M. E. and Boyer, J. S. Transpiration- and growth-induced water potentials in maize. *Plant Physiol.*, 1984, **74**, 882–889.
99. Wiebel, E. R. *Morphometry of the Human Lung*. Academic Press, New York, 1963.
100. Young, T. Hydraulic investigations subservient to an intended Croonian lecture on the motion of the blood. *Philos. Trans. Roy. Soc.*, 1808, **98**, 164–186.
101. Zamir, M. Shear forces and blood vessel radii in the cardiovascular system. *J. Gen. Physiol.*, 1977, **69**, 449–462.
102. Zamir, M. and Bigelov, D. C. Cost of departure from optimality in arterial branching. *J. Theor. Biol.*, 1984, **109**, 401–409.
103. Zamir, M. Distributing and delivering vessels of the human heart. *J. Gen. Physiol.*, 1988, **91**, 725–735.
104. Zenin, O. K., Kizilova, N. N. and Philippova, E. N. Studies on the structure of human coronary vasculature. *Biophysics*, 2007, **52**, 499–503.
105. Zhi, W., Ming, Zh. and Qi-Xing, Y. Modeling of branching structures of plants. *J. Theor. Biol.*, 2001, **209**, 383–394.
106. Zialalov, A. A. *Physiological and Thermodynamic Aspects of Water Transport in Plants*. Nauka, Moscow, 1985 (in Russian).
107. Zolkevich, V. N., Gusev, N. A., Kaplya, N. A. et al. *Water Exchange in Plants*. Nauka, Moscow, 1989 (in Russian).

Vedeliku kaugtransport taimedes

Natalya N. Kizilova

On esitatud lühiülevaade taimedes toimuvast vedeliku kaugtranspordi ja signaalide levikuga seotud termodünaamika ning vedelike dünaamika probleemidest. On mõõdetud lehesoonte geomeetrilisi parameetreid ja saadud üldised seosed lehesoonte läbimõõdu ning pikkuse ja soonte hargnevusnurkade ning vastavate drenaaživäljade vahel. Samad seosed olid varem saadud imetajate ja inimeste arteriaalse ning bronhiaalse süsteemi soonte ja puutüvedes, nende võrades ning juurestikes ja jõgede vesikondades esinevate hargnevuste kohta. Optimaalsete võrgustike kontseptsioon, mis tagab vedeliku ülekande minimaalse koguenergia kuluga, võimaldab aru saada looduslike transpordisüsteemide ülesehituse ühtsetest põhialustest. On esitatud läbilaskvate ja mitteläbilaskvate seintega optimaalsete soonte ning nende hargnevussüsteemide vastavad mudelid koos kommentaaridega.